An efficient control transition scheme between stabilization and tracking task of a MAGLEV platform enabling active vibration compensation

Daniel Wertjanz, Ernst Csencsics and Georg Schitter

***Abstract*— This paper proposes an efficient handing over from the internal stabilization to the external tracking control of a magnetically levitated platform, enabling precise robot-based measurements of free form surfaces. The platform prototype comprises two different sensor systems. The internal sensor system is used to stabilize the platform in a free-floating position with respect to the supporting frame (internal position control), while the external one enables the active compensation of disturbing vibrations by tracking a sample surface (external position control). Based on a cross-fading error gain, the control structure for each out-of-plane DoF comprises a single PID position controller for both control tasks of the platform. Measurement results demonstrate the platform's capability of performing a simultaneous control transition in the out-of-plane DoFs, while it is stabilized in-plane. Different transition functions are applied to the cross-fading error gain. The findings show that a minimum jerk trajectory performs best regarding transition time and cross-coupling. Using this minimum jerk transition, the translational and rotational positioning errors in the three stabilizing in-plane DoFs are kept below 137 nm rms and 2.05 µrad rms, respectively.**

I. Introduction

Modern industrial manufacturing systems have a continuously growing demand in precision and throughput [1]. Besides novel production technologies, high-precision in-line measurements are considered as a key factor for future production [2]. Particularly for the surface inspection of free forms, such as car bodies [3], flexible and versatile inline measurement systems will be of great importance in the upcoming decades [4]. Robot-based measurement systems can offer the required flexibility and have the potential to significantly increase the reliability and quality of produced goods, by boosting throughput at the same time. Most high-precision measurement systems, operating at the sub-micrometer level, need to be properly aligned with respect to the sample surface and are typically highly sensitive to vibrations. Such measurement systems are usually applied in a vibration-free environment, which is, however, in complete contrary to the vibration-prone environment of an industrial manufacturing plant. By causing motion blur between the measurement tool and the sample in 6 degrees of freedom (DoFs) [5], environmental floor vibrations disturb measurements at the micrometer scale [6]. Therefore, the integration of a flexible robot-based high-precision measurement system directly in a production line is considered as a major challenge.

Recently, a robot-based approach has been proposed [7]–[10]. Used as a robot end-effector, a magnetically levitated (MAGLEV) positioning platform carries a measurement tool and maintains a constant distance and orientation between the sample surface and the measurement tool on the platform by means of feedback control. Thus, an artificially stiff link between sample and tool is established, actively compensating for disturbing environmental vibrations. However, due to the implemented permanent magnet assembly for gravity compensation, the proposed platform design is limited to horizontal operation orientation. As a first step towards enabling measurements of free form surfaces, a six DoF MAGLEV positioning platform with arbitrary operation orientation has been developed in [11]. Based on a symmetric actuation system using voice coil actuators (VCAs) and internal position sensors, the platform is capable of being positioned with respect to the supporting frame and shows an orientation-independent system performance.

The contribution of this paper is the implementation of an efficient handing over between the internal stabilization and the tracking of the sample surface.

The system concept of high precision robot-based surface measurements is described in Section II. In Section III the prototype system is presented. Based on an identification of the system dynamics, the internal and external position control is designed in Section IV The proposed transition scheme is described in Section V, while the system performance is evaluated in Section VI. Finally, Section VII concludes the paper.

II. System Concept

The system concept of a MAGLEV platform enabling robot-based inline measurements of free forms comprises two different sensor systems for two different control tasks and is illustrated in Fig. 1. Initially, the MAGLEV platform needs to be stabilized in a desired free-floating position with respect to the supporting frame (internal position control), when the robot arm is repositioning and approaching a sample surface (Fig. 1a).

Once the external tracking sensors (TS) are in range, disturbing environmental vibrations are actively compensated during a surface measurement by tracking the sample surface and maintaining a constant distance and orientation between the measuring tool and the sample (external position control), as depicted in Fig. 1b. Therefore, the requirement of an efficient handing over between the internal and external position control task in Fig. 1 arises. However, two major aspects need to be considered. On the one hand, during the transition from internal to external position control and vice versa, unintended transients in the platform position need

The authors are with the Christian Doppler Laboratory for Precision Engineering for Automated In-Line Metrology, Automation and Control Institute (ACIN), Technische Universität Wien, 1040 Vienna. Corresponding author: wertjanz@acin.tuwien.ac.at

Post-print version of the paper: D. Wertjanz, E. Csencsics, and G. Schitter, "An efficient control transition scheme between stabilization and tracking task of a MAGLEV platform enabling active vibration compensation", *2020 IEEE/ASME International Conference on Advanced Intelligent Mechatronics (AIM)*, 2020. DOI: 10.1109/AIM43001.2020.9158924

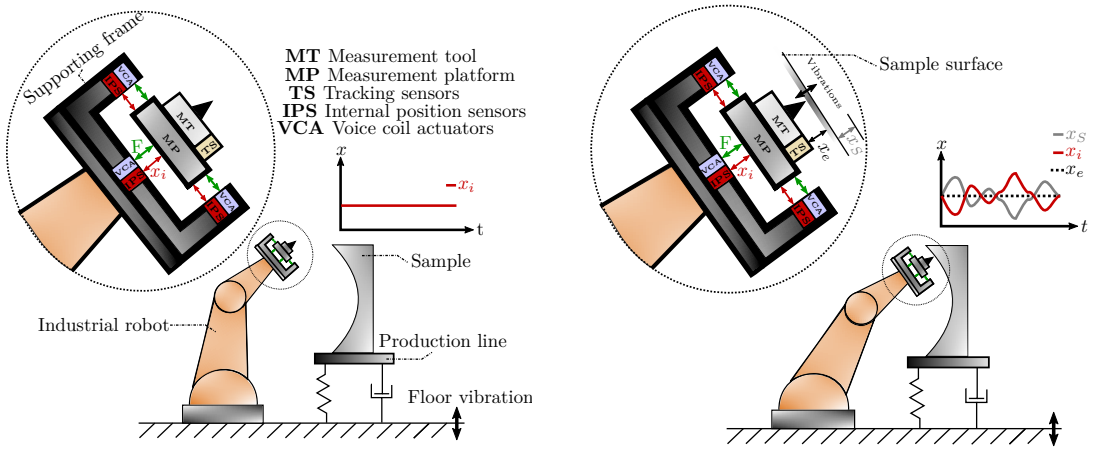

(a) Repositioning task.

(b) In-line surface measurement.

Fig. 1: A MAGLEV platform enabling robot-based high precision in-line measurements of free form surfaces. a) When the robot is repositioning and approaching the sample surface section to be inspected, the platform needs to be stabilized in a free-floating position with respect to its supporting frame using the internal position sensors (IPS). b) To actively isolate both the measurement tool and the sample, the platform is required to maintain a constant distance and orientation relative to the sample surface by use of the tracking sensors (TS).

to be avoided to prevent a sensitive measurement tool from damage. On the other hand, a fast transition is desired for reasons of efficiency, keeping the overall measurement time at the surface section of interest as low as possible.

III. System Description

A. Platform design

Figure 2 shows the MAGLEV platform prototype which is capable of being positioned in arbitrary orientations of the system. [11]. The system includes a custom-made internal position sensor system (IPS), based on six optical proximity sensors (HSDL-9100, Avago Technologies, San Jose, California, United States), to measure the platform position in all DoFs with respect to the supporting frame. The IPS shows an improved rms position noise of about 75 nm and 1.2 µrad in the translational and rotational DoFs, respectively, than presented in [11]. The bandwidth of the IPS is 10 kHz. The system comprises eight VCAs (VCAR0087-0062-00A, Supt-Motion, Suzhou, China) to a actuate the platform in six DoFs. To apply a desired current to each VCA, a custom-made analog PI current controller, designed for a bandwidth of 10 kHz, and amplifier (OPA544T, Burr-Brown, Tucson, Arizona, United States) is used. Each VCA is capable of applying a continuous force of 20 N to the platform. The actuation range is determined by the actuator placement and the air gap of the VCA. However, an actuation of about ±180 µm and ±2 mrad in the translational and rotational DoFs, respectively, is achieved.

B. Integration of tracking sensors

To enable a highly precise determination of the out-of-plane distance and orientation relative to a sample surface, a tracking sensor system (TS) is required. Therefore, three capacitive displacement sensors (CSH05, Micro-Epsilon, Ortenburg, Germany), with a position noise of about 15 nm rms over a range of 400 µm and a bandwidth 6 kHz, are used and placed on top of the platform (Fig. 2). Due to the placement of the TS on the same axes as the three internal out-of-plane sensors, the simple relation

$$z_i + z_0 = -z_e \tag{1a}$$
$$\phi_{x,i} = -\phi_{x,e} \tag{1b}$$
$$\phi_{x,i} = -\phi_{y,e}, \tag{1c}$$

between the internal and external out-of-plane positions is obtained, with z_0 being a constant offset between the measured z-position values.

IV. Control Design

Based on the floating mass model of the MAGLEV platform and using the signal of the IPS as feedback, a low-bandwidth PID controller for each DoF is designed and the system dynamics are identified in a closed-loop manner [11]. Using the identified system dynamics, exemplary shown by $G_{z,i}$ in Fig. 3 for the internal position z_i, the control parameters are adapted in a loop shaping approach [12] to achieve the highest possible position control bandwidth (solid black). At this point, the platform can be stabilized and positioned in 6 DoFs with respect to the supporting frame (internal position control). Each of the six internal is designed for a closed-loop control bandwidth of about 130 Hz.

Post-print version of the paper: D. Wertjanz, E. Csencsics, and G. Schitter, "An efficient control transition scheme between stabilization and tracking task of a MAGLEV platform enabling active vibration compensation", *2020 IEEE/ASME International Conference on Advanced Intelligent Mechatronics (AIM)*, 2020. DOI: 10.1109/AIM43001.2020.9158924

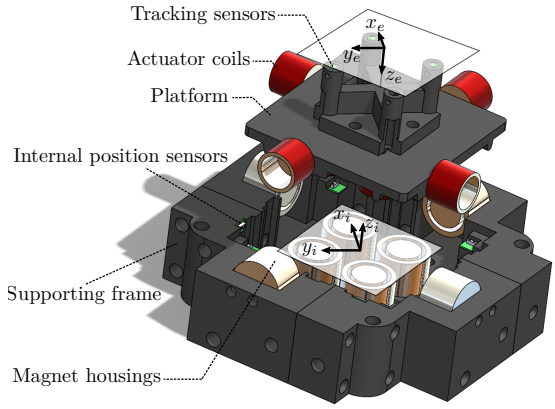

Fig. 2: Exploded view of MAGLEV platform prototype. VCAs are used to actuate the platform in six DoFs. Internal position sensors determine the platform position with respect to the supporting frame. A set of three tracking sensors enables the measurement of the out-of-plane position and orientation relative to a sample surface.

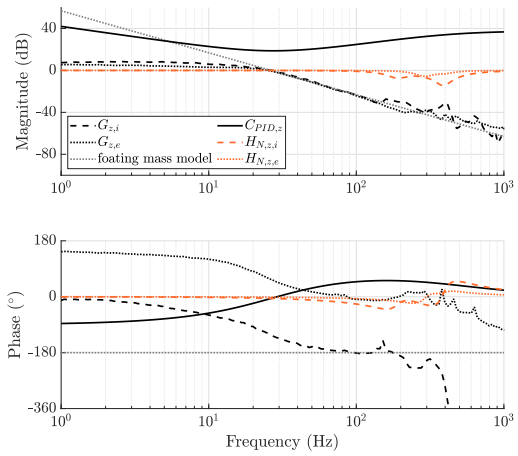

Fig. 3: Identified system dynamics and controller design of degree of freedom (DoF). Good accordance between the floating mass model and the measured dynamics of the internal and external position ($G_{z,i}$ and $G_{z,e}$) is achieved. $C_{PID,z}$ indicates the designed PID controller, while $H_{N,z,i}$ and $H_{N,z,e}$ represent the individual notch filters.

To design the external position control, the system identification approach is repeated using the external position signals of the TS as feedback. According to Eq. 1, the dynamics of internal and external out-of-plane positions are the same except for the sign, which can be seen by the phase shift of almost 180° between $G_{z,e}$ and $G_{z,i}$ (Fig. 3). Thus, by inverting the sign of the external position signal, the same PID parameters for the internal and external position control can be used. However, due to the placement of the tracking sensors closer to the platform's center, measured structural modes of the moving platform by the TS at frequencies higher than 160 Hz differ from the dynamics observed by the IPS. Therefore, individually tailored notch filters $H_{n,z,i}$ and $H_{n,z,e}$ are included in design of the internal and external position control to ensure robustness. The two obtained controller designs for the translational DoF z are given by

$$C_{z,i} = C_{PID,z} H_{N,z,i} \tag{2a}$$
$$C_{z,e} = C_{PID,z} H_{N,z,e}. \tag{2b}$$

The same scheme is applied to the two out-of-plane DoFs ϕ_x and ϕ_y. Each of the three external position controller is designed for a closed-loop control bandwidth of about 130 Hz. Now, the system prototype presented in Fig. 2 is capable of tracking a sample surface in the three out-of-plane DoFs z, ϕ_x and ϕ_y, while the platform can be stabilized in-plane (x, y and ϕ_z).

V. Control Transition Scheme

A. Methodology

Considering the desired system concept with the MAGLEV platform carrying a measurement tool and mounted as an end effector to an industrial robot arm, an efficient transition between the internal and external position control is required, once the TS are in range (see Fig. 1). This is done by inverting the sign of the external position signal and using the same PID parameters for control of the internal and external out-of-plane position pairs $\{z_i, z_e\}$, $\{\phi_{x,i}, \phi_{x,e}\}$ and $\{\phi_{y,i}, \phi_{y,e}\}$ (see Section IV). The transition is implemented of a time-dependent cross-fading error gain $\gamma \in [0, 1]$, as exemplary shown for one DoF in Fig. 4. Let γ be defined as

$$\gamma = \begin{cases} 0 & \text{if } t \leq 0 \\ 1 & \text{if } t \geq T \\ \gamma(t) & \text{otherwise,} \end{cases} \tag{3}$$

with T being the transition time between internal and external position control.

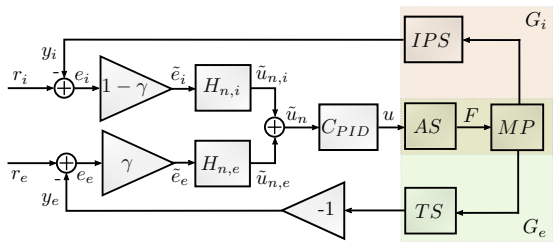

Fig. 4: Control transition scheme in one DoF between internal stabilization and tracking a sample using a cross-fading error gain $\gamma \in [0, 1]$ and a single PID position controller.

Assuming $\gamma = 0$, the loop gain of the proposed control structure is $L(\gamma)|_{\gamma=0} = L_i = C_{PID} H_{N,i} G_i = C_i G_i$, which

Post-print version of the paper: D. Wertjanz, E. Csencsics, and G. Schitter, "An efficient control transition scheme between stabilization and tracking task of a MAGLEV platform enabling active vibration compensation", *2020 IEEE/ASME International Conference on Advanced Intelligent Mechatronics (AIM)*, 2020. DOI: 10.1109/AIM43001.2020.9158924

means that the internal position control is active and the platform is stabilized in a free-floating position with respect to the supporting frame. The loop gain for $\gamma = 1$, meaning that the external position control is enabled, is $L(\gamma)|_{\gamma=1} = L_e = C_{PID}H_{N,e}G_e = C_eG_e$. For any $\gamma \in [0,1]$, the effective loop gain results in

$$\begin{aligned} L(\gamma) &= (1-\gamma)H_{n,i}C_{PID}G_i + \gamma H_{n,e}C_{PID}G_e \\ &= (1-\gamma)L_i + \gamma L_e, \end{aligned} \tag{4}$$

which is stable since it is a weighted superposition of the two stable loop gains L_i and L_e with the same cross-over freuqency.

B. Transition functions

As discussed in Section II, a fast transition from the internal to external position control, which does not cause transients in the platform position, is desired. Moreover, during a performed handing over between the two control tasks, the coupling to the stabilizing in-plane DoFs is required to be low. Therefore, different transition functions are considered and compared. Regarding the proposed control structure in Fig. 4, a transition from internal to external position control is equivalent to a simultaneous but opposed change in the reference signals r_i and r_e. Thus, it is obvious that a smooth slope for the cross-fading error gain $\gamma(t)$ is desirable, in order to avoid any transients in the position signals. Besides a lowpass filtered step $\gamma_{lp}(t)$ and a ramp-function $\gamma_{ramp}(t)$, a minimum jerk trajectory $\gamma_{mj}(t)$ [13], [14] is considered for the slope of the cross-fading error gain. This minimum jerk trajectory is a fifth order polynomial which minimizes the cost function $J = \int_0^T \frac{1}{2}\left(\frac{\partial u}{\partial t}\right)^2 dt$, with u being the controller output of Fig. 4. The transition functions are defined as

$$\gamma_{ramp}(t) = \frac{t}{T} \tag{5a}$$

$$\gamma_{lp}(t) = 1 - e^{-t/(5T)} \tag{5b}$$

$$\gamma_{mj}(t) = 6\left(\frac{t}{T}\right)^5 - 15\left(\frac{t}{T}\right)^4 + 10\left(\frac{t}{T}\right)^3, \tag{5c}$$

for $t \in [0,T]$. All three functions in Eq. 5 converge for $T \to 0$ to the step function and are shown in Fig. 5 (black).

To determine the order of magnitude of the minimum achievable transition time T, which still ensures a smooth transition and no transients or overshooting in the platform position, the proposed transition scheme is simulated for DoF z. Therefore, the identified system dynamics and the controller design presented in Fig. 3 are used. Simulation results for all three transition functions and a transition time of $T = 50\,\mathrm{ms}$ are illustrated in Fig. 5 (red). Moreover, a simulation results for a step-wise transitions are shown. For reasons of comparability the signal $1 - \frac{e_{z,e}(t)}{e_{z,e,0}}$ is shown, with $\frac{e_{z,e}(t)}{e_{z,e,0}}$ being the normalized position error and $e_{z,e,0}$ the initial position error of z_e. It is obvious that applying a step function to $\gamma(t)$ is not expedient in terms of the required smoothness of the position slope. Therefore, it is

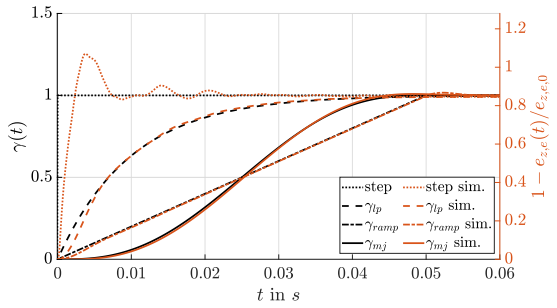

Fig. 5: Simulation results of the external position z_e for the transition functions in Eq. 5 and $T = 50\,\mathrm{ms}$.

not considered in the subsequent performance evaluation. According to the simulation results for a transition time of $T = 50\,\mathrm{ms}$, slight overshooting in the position error $e_{z,e}(t)$ results for a ramp-wise transition.

VI. Evaluation of System Performance

The transition scheme presented in the previous section is implemented for the three out-of-plane DoFs z, ϕ_x and ϕ_y. The performance regarding a possible overshoot in the platform's out-of-plane position is evaluated, with the cross-fading error gain $\gamma(t)$ following the different transition functions in Eq. 5. Therefore, the platform is positioned in a free-floating position using the internal position control, such that the initial external position and orientation error between the platform and a stationary sample surface is $e_{z,e,0} = 50\,\mu\mathrm{m}$ and $e_{\phi_{x,e,0}} = e_{\phi_{y,e,0}} = 350\,\mu\mathrm{rad}$, respectively.

The transition from internal to external position control in the three DoFs is performed simultaneously. Table I summarizes the results regarding overshoot in the position signals for decreasing transition times T. According to these experimental results, $T = 50\,\mathrm{ms}$ is considered as the minimum transition time for the minimum jerk and low pass transition. Due to higher frequency components in the spectrum of the ramp function and the limited position control bandwidth of about $130\,\mathrm{Hz}$, it is clearly observable that a ramp-wise transition is not expedient because it causes overshoot in the position signal for all applied transition times. In Fig. 6 the simulation and measurement results of the decreasing external error $e_{z,e}$ over the transition time of $T = 50\,\mathrm{ms}$ are compared. Good accordance between simulated (dotted) and measured (solid) position signal can be seen.

Figure 7 shows the results of applying the low pass filtered step and the minimum jerk trajectory of Eq. 5 using the minimum transition time of $T = 50\,\mathrm{ms}$. In the left column the decreasing external and opposingly increasing internal out-of-plane position errors are shown for initial external position and orientation errors of $e_{z,e,0} = 50\,\mu\mathrm{m}$ and $e_{\phi x,e,0} = e_{\phi y,e,0} = 350\,\mu\mathrm{rad}$, respectively. When applying the low-pass filtered step to the cross-fading error gain $\gamma(t)$, transients in the position signal of the rotational DoFs ϕ_x

Post-print version of the paper: D. Wertjanz, E. Csencsics, and G. Schitter, "An efficient control transition scheme between stabilization and tracking task of a MAGLEV platform enabling active vibration compensation", *2020 IEEE/ASME International Conference on Advanced Intelligent Mechatronics (AIM)*, 2020. DOI: 10.1109/AIM43001.2020.9158924

TABLE I: Relative overshoot in % using different cross-fading error gain slopes $\gamma(t)$ and transition times T (initial position errors $e_{z,e,0} = 50\,\mu\text{m}$, $e_{\phi_{x,e,0}} = e_{\phi_{y,e,0}} = 350\,\mu\text{rad}$).

	Overshoot of $z_e/\phi_{x,e}/\phi_{y,e}$ in %		
T (ms)	$\gamma_{\mathbf{ramp}}$	$\gamma_{\mathbf{lp}}$	$\gamma_{\mathbf{mj}}$
500	0.3 / 0.5 / 0.4	0 / 0 / 0	0 / 0 / 0
250	0.6 / 0.9 / 0.8	0 / 0 / 0	0 / 0 / 0
100	1.3 / 1.9 / 1.9	0 / 0 / 0	0 / 0 / 0
50	2.5 / 3.2 / 4.0	0 / 1.2 / 1.1	**0.2 / 0.4 / 0.5**
40	3.1 / 4.4 / 5.1	0.3 / 1.4 / 2.3	0.4 / 0.9 / 1.6
30	4.0 / 5.6 / 7.0	0.6 / 1.7 / 5.9	0.9 / 2.3 / 4.9

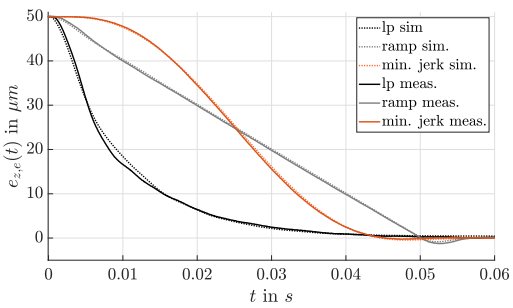

Fig. 6: Measurement results for the external position error $e_{z,e}(t)$ using the different transition functions (Eq. 5) and a transition time of $T = 50\,\text{ms}$. Good accordance between the measured slopes (solid lines) of $e_{z,e}(t)$ and the simulation results (dotted lines) can be observed.

and ϕ_y can be seen. In contrast, applying the minimum jerk trajectory results in a significantly smoother slope of the out-of-plane position and orientation errors. The rms position errors in the stabilizing in-plane DoFs x, y and ϕ_z during the transition, shown in the right column of Fig. 7 are evaluated as a measure of cross-coupling. It can be clearly seen that, using the minimum jerk transition function γ_{mj} results in significantly lower positioning errors in the stabilizing in-plane DoFs. Table II summarizes the in-plane rms position errors shown in Fig. 7 and encourage this statement. It can be noted that the minimum jerk transition performs best regarding transition time and cross-coupling.

TABLE II: Cross-coupling to in-plane position during a control transition different cross-fading error gain slopes $\gamma(t)$ and a transition time of $T = 50\,\text{ms}$.

	In-plane rms position errors	
Pos.	$\gamma_{\mathbf{lp}}$	$\gamma_{\mathbf{mj}}$
$e_{x,i}$	91 nm	79 nm
$e_{y,i}$	145 nm	137 nm
$e_{\phi z,i}$	2.4 µrad	2.05 µrad

In summary, the experimental results successfully demonstrate the stability of the proposed transition scheme between the internal and external position control.

VII. Conclusion

In this paper the development and validation of a control transition scheme for a MAGLEV platform enabling high precision robot-based measurements of free form surfaces are presented. The prototype system comprises two different sensor systems for two different control tasks. The proposed scheme enables an efficient transition between i) the platform's internal position control, which is used to stabilize the platform in 6 DoFs with respect to the supporting frame, and ii) the external position control, which actively compensates for disturbing vibrations during a conceptual measurement by maintaining the measurement platform at a constant distance and orientation relative to a sample surface. Based on a cross-fading error gain, the proposed transition scheme is implemented for each out-of-plane DoF, using a single PID position controller for both, the internal and external position control. Therefore, for each DoF a transition between internal and external position control is equivalent to a simultaneous but opposed change in the references for the two individual positions. Meeting the requirements of low transition times for reasons of efficiency and, at the same time, preventing a conceptual measurement tool from damage by avoiding transients in the platform's position, the experimental results in this work propose the cross-fading error gain to follow a minimum jerk trajectory. Using this minimum jerk transition, the platform prototype shows a negligible overshoot in the out-of-plane positions z, ϕ_x and ϕ_y for transition times down to $50\,\text{ms}$ and a stationary sample surface. Thereby, translational and rotational positioning errors in the stabilizing in-plane DoFs lower than $137\,\text{nm}$ rms and $2.05\,\mu\text{rad}$ rms are achieved, respectively.

Acknowledgment

The financial support by the Christian Doppler Research Association, the Austrian Federal Ministry for Digital and Economic Affairs, and the National Foundation for Research, Technology and Development, as well as MICRO-EPSILON MESSTECHNIK GmbH & Co. KG and ATENSOR Engineering and Technology Systems GmbH is gratefully acknowledged.

References

[1] T. Uhrmann, T. Matthias, M. Wimplinger, J. Burggraf, D. Burgstaller, H. Wiesbauer, and P. Lindner. Recent progress in thin wafer processing. In *2013 IEEE International 3D Systems Integration Conference (3DIC)*, pages 1–8, 2013.

[2] D. Imkamp, R. Schmitt, and J. Berthold. Blick in die Zukunft der Fertigungsmesstechnik - Die VDI/VDE-GMA Roadmap Fertigungsmesstechnik 2020. *Technisches Messen*, 10(79), 2012.

[3] Arjun Yogeswaran and Pierre Payeur. 3d surface analysis for automated detection of deformations on automotive body panels. In *New Advances in Vehicular Technology and Automotive Engineering*. IntechOpen, 2012.

[4] Heinrich Schwenke, Ulrich Neuschaefer-Rube, Tilo Pfeifer, and Horst Kunzmann. Optical methods for dimensional metrology in production engineering. *CIRP Annals*, 51(2):685 – 699, 2002.

[5] Colin G. Gordon. *Generic Vibration Criteria for Vibration-Sensitive Equipment*. Colin Gordon & Associates, 1999.

[6] Rudolf Saathof, Markus Thier, Reinhard Hainisch, and Georg Schitter. Integrated system and control design of a one dof nano-metrology platform. *Mechatronics*, 47:88 – 96, 2017.

Post-print version of the paper: D. Wertjanz, E. Csencsics, and G. Schitter, "An efficient control transition scheme between stabilization and tracking task of a MAGLEV platform enabling active vibration compensation", *2020 IEEE/ASME International Conference on Advanced Intelligent Mechatronics (AIM)*, 2020. DOI: 10.1109/AIM43001.2020.9158924

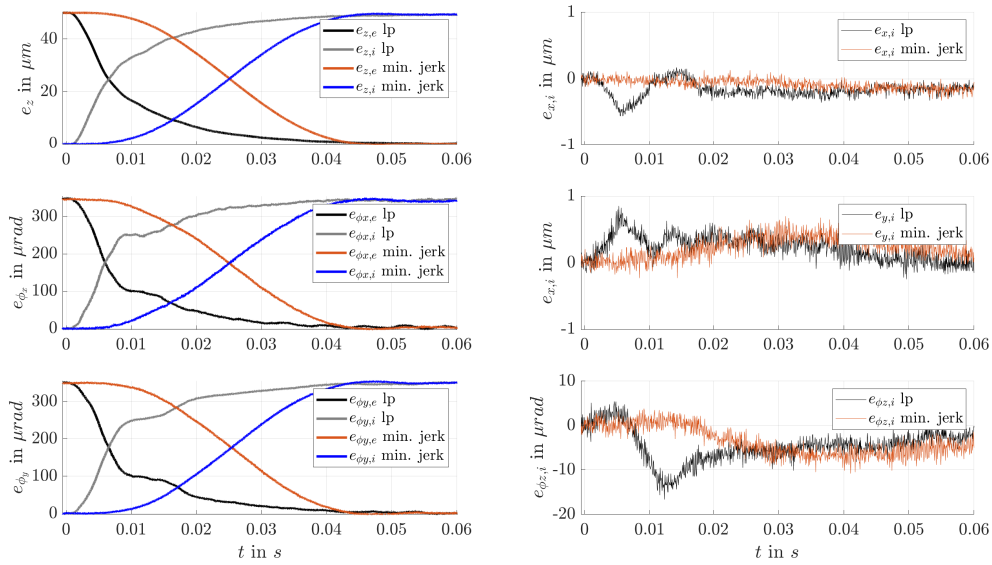

Fig. 7: Positioning errors in all DoFs during a control transition using the low pass filtered step and the minimum jerk trajectory of Eq. 5 with $T = 50\,\mathrm{ms}$. The left column shows the decreasing external and the increasing internal position error. During the control transition the platform is stabilized in-plane with position errors shown in the right column. Lower cross-coupling to the stabilizing in-plane DoFs can be observed using the minimum jerk transition.

[7] M. Thier, R Saathof, R Hainisch, and G. Schitter. Vibration compensation platform for robot-based nanoscale measurements. *15th International Conference of the EUSPE*, pages 59–71, 2015.

[8] M. Thier, R Saathof, E. Csencsics, R Hainisch, A. Sinn, and G. Schitter. Design and control of a positioning system for robot-based nanometrology. *at- Automatisierungstechnik*, 63:727 – 738, 2015.

[9] Ruijun Deng, Rudolf Saathof, J.W. Spronck, S.A.J. Hol, and Robert H. Munnig Schmidt. Integrated 6-dof lorentz actuator with gravity compensator for precision positioning. *22nd International Conference on Magnetically Levitated Systems and Linear Drives (MAGLEV)*, 2014.

[10] M. Thier, R. Hainisch, G. Schitter, and R. Saathof. Metrology platform to enable in-line nanometrology. *Industrial Technologies, Amsterdam, The Netherlands*, 2016.

[11] D. Wertjanz, E. Csencsics, J. Schlarp, and G. Schitter. Design and control of a maglev platform for positioning in arbitrary orientations. In *IEEE/ASME International Conference on Advanced Intelligent Mechatronics*, 2020. submitted.

[12] E. Csencsics and G. Schitter. Parametric pid controller tuning for a fast steering mirror. In *2017 IEEE Conference on Control Technology and Applications (CCTA)*, pages 1673–1678, 2017.

[13] T. Yamaguchi, M. Hirata, and J.C.K. Pang. *High-Speed Precision Motion Control*. CRC Press, 2017.

[14] Paul Lambrechts, Matthijs Boerlage, and Maarten Steinbuch. Trajectory planning and feedforward design for electromechanical motion systems. *Control Engineering Practice*, 13(2):145 – 157, 2005.

Post-print version of the paper: D. Wertjanz, E. Csencsics, and G. Schitter, "An efficient control transition scheme between stabilization and tracking task of a MAGLEV platform enabling active vibration compensation", *2020 IEEE/ASME International Conference on Advanced Intelligent Mechatronics (AIM)*, 2020. DOI: 10.1109/AIM43001.2020.9158924